E2-2002-37

G. N. Afanasiev[1], V. M. Shilov, Yu. P. Stepanovsky[2]

# NUMERICAL AND ANALYTIC TREATMENT OF THE SMOOTHED TAMM PROBLEM

Submitted to «Journal of Physics A»

[1]E-mail: afanasev@thsun1.jinr.ru
[2]Institute of Physics and Technology, Kharkov, Ukraine

# 1 Introduction

In 1934-1937, P.A. Cherenkov performed a series of experiments where he observed the radiation induced by $\gamma$ quanta propagating in water. He associated this radiation with the electrons knocked out by photons from the medium atoms. S.I. Vavilov, Cherenkov's teacher, attributed observed radiation to the deceleration of electrons [1]. At that time, P.A. Cherenkov agreed with S.I. Vavilov concerning the nature of the radiation. According to him [2], "All the above-stated facts unambigously testify that the nature of the $\gamma$ luminiscence is due to the electromagnetic deceleration of electrons moving in a fluid. The facts that $\gamma$ luminiscence is partially polarized and that its brightness has a highly pronounced asymmetry, strongly resemble the similar picture for the bremsstrahlung of fast electrons in the Roentgen region. However, in the case of the $\gamma$ luminiscence, the complete theoretical interpretation is encountered with a number of difficulties." (our translation from Russian). In 1937, Tamm and Frank showed ( the nice exposition of this theory may be found, e.g., in [3]) that a charge uniformly moving in medium should radiate if its velocity $v$ is greater than the light velocity in medium $c_n$. Since this theory corresponds to unbounded charge motion in medium, the Cherenkov cone attached to a moving charge is infinite. In 1939, Tamm ([4]) considered the radiation of a charge which is instantly accelerated at some moment of time $t_1$, moves uniformly in the time interval $t_1 < t < t_2$ with the velocity $v > c_n$, and is instantly decelerated at the moment $t = t_2$. For $t < t_1$ and $t > t_2$, the charge is at rest. Tamm obtained the remarkably simple formula describing the angular-frequency distribution of radiation. Due to the instantaneous charge acceleration, the Cherenkov shock wave is created instantly as well, and there is no possibility to observe its formation. To remove this drawback, the charge motions similar to that shown in Fig. 1(a), were considered in [5] and [6], in the time representation. It was shown there that a complex consisting of the Cherenkov shock wave and the shock wave closing the Cherenkov cone (and not coinciding with the bremsstrahlung shock wave) is created at the moment the charge velocity coincides with the light velocity in medium. Time evolution of this complex before and after termination of a charge motion was also studied there.

After appearance of the Tamm-Frank theory, P.A. Cherenkov expressed his solidarity with it [7]. The Vavilov explanation of the Cherenkov effect has given rise to a number of attempts (see, e.g., [8,9]) in which the radiation described by the Tamm formula was attributed to the interference of bremsstrahlung (BS) shock waves arising at the beginning and termination of motion. The Tamm problem, simultaneously in the time and spectral representations was reconsidered in [10]. In the time representation, it was shown that, in some interval of time, there is a shock wave associated with the beginning of motion and the Cherenkov shock wave, and there is no shock wave associated with the termination of motion (it is not still appeared). Thus, at least in some time interval, the Cherenkov shock wave cannot be attributed to the interference of the above BS shock waves. In the spectral representation, the motion law shown in Fig. 1 (a) was considered in [10]. From the analytic solution found

there, it was shown that the accelerated and decelerated parts of a charge trajectory do not contribute to the total radiation intensity when their lengths tend to zero (despite the infinite acceleration and deceleration at the start and end of motion). This means that the original Tamm problem, as a limiting case of motion shown in Fig. 1 (a), describes charge motion on a finite space interval without recourse to the instantaneous acceleration and deceleration. Despite the fact that for the motion shown in Fig.1 (a) there are no jumps of the charge velocity and the acceleration (deceleration) is everywhere finite, there are jumps of acceleration at the moments of time corresponding to the start and end of motion and at the time moments when the acceleration (deceleration) motion meets with the uniform one. The time derivatives of acceleration are infinite at these moments of time. It was not clear to authors of [10], whether these jumps contribute to the radiation intensity.

The goal of this consideration is to remove this insufficiency. For this aim, we consider the charge motion law for which all time derivatives are everywhere finite and do not exhibit jumps (Fig. 1 (b,c)). Despite this, the charge position remains within a finite space interval. It is shown that radiation intensities corresponding to Fig. 1(a) strongly resemble the ones corresponding to Fig.1 (b,c) when the parameters of motion laws are properly adjusted. Therefore, jumps of acceleration are not essential, and one can apply analytic radiation intensities found in [10] for the motion shown in Fig.1 (a) to the qualitative analysis of the motions depicted in Fig.1 (b,c).

The plan of our exposition is as follows. In section 2, main computational formulae are given, and the approximations used are discussed. The properties of motion laws shown in Figs. 1 (b) and (c) are studied in section 3. Numerical calculations presented in section 4 show that: i) for the motion laws of Fig. 1 (b) and (c), the radiation intensity falls almost instantly for angles exceeding the Cherenkov angle; ii) for the motion corresponding to a zero final velocity (a moving charge is absorbed in medium), the maximum of the radiation intensity is always at the Cherenkov angle defined by $\cos\theta_c = 1/\beta_0 n$ ($n$ is the medium refractive index and $\beta_0$ is the initial velocity) despite the highly non-uniform character of motion; iii) the frequency distribution of the radiation (obtained by integration of the angular frequency distribution over the solid angle) is proportional to the frequency (i.e., exactly the same as in the Tamm problem). In section 5, analytic formulae obtained in [10] and describing the motion laws similar to that of Fig. 1(a) are rewritten in terms of elementary functions. It is shown that: i) instantaneous decrease of the radiation intensity for $\theta > \theta_c$ is due to the interference of uniform and non-uniform motions; ii) the maximum of the radiation intensity is always at $\theta = \theta_c$; iii) the appearance of two Cherenkov angles defined by $\cos\theta_1 = 1/\beta_1 n$ and $\cos\theta_2 = 1/\beta_2 n$ should be expected for the motion with the initial velocity $\beta_1$ and the final one $\beta_2$ (where both $\beta_1$ and $\beta_2$ are greater than $1/n$). These facts were admitted in [10], but no satisfactory explanation was given there. The discussion of the results obtained and their relation to the original Cherenkov experiments is given in section 6. Finally, in section 7, we summarize the main results of this treatment.

## 2 Preliminairies

Consider a point -like charge moving in medium with parameters $\epsilon$ and $\mu$. Let the charge velocity and trajectory be $\vec{v}(t)$ and $\vec{\xi}(t)$. For the definiteness, let it move along the $z$ axis. The flux of energy through the observation sphere $S$ of the radius $r$ per unit frequency and per unit solid angle is given by

$$\sigma(\theta,\omega) = \frac{d^2\mathcal{E}}{d\omega\Omega} = \frac{e^2\mu n k^2 \sin^2\theta}{4\pi^2 c}(I_c I_c' + I_s I_s'), \tag{2.1}$$

where

$$I_c = \int \frac{v d\tau}{R^2}(\cos\psi - \frac{\sin\psi}{k_n r R}), \quad I_s = \int \frac{v d\tau}{R^2}(\sin\psi + \frac{1}{k_n R r}\cos\psi),$$

$$I_c' = \int \frac{v d\tau}{R^3}(1 - \frac{\xi}{r}\cos\theta)(\cos\psi - 3\frac{\sin\psi}{k_n R r} - 3\frac{\cos\psi}{k_n^2 R^2 r^2}),$$

$$I_s' = \int \frac{v d\tau}{R^3}(1 - \frac{\xi}{r}\cos\theta)(\sin\psi + 3\frac{\cos\psi}{k_n R r} - 3\frac{\sin\psi}{k_n^2 r^2 R^2}),$$

$$\psi = \omega\tau + k_n r(R-1), \quad R = [1 + \frac{\xi^2}{r^2} - 2\frac{\xi}{r}\cos\theta]^{1/2}, \quad k_n = kn,$$

$r$ and $\theta$ define radial and angular positions of the observation point, and $n = \sqrt{\epsilon\mu}$ is the medium refractive index. When obtaining (2.1), it is implicitly suggested that the charge motion interval lies entirely inside the observation sphere $S$.

However, Eq. (2.1) is not suitable for practical applications and the qualitative analysis of radiation intensities. Therefore, some approximations are needed. We briefly enumerate them:

1. In the wave zone, where $kr >> 1$, one can disregard terms of the order $1/kr$ and higher, thus obtaining

$$I_c = \int \frac{v d\tau}{R^2}\cos\psi, \quad I_s = \int \frac{v d\tau}{R^2}\sin\psi,$$

$$I_c' = \int \frac{v d\tau}{R^3}(1 - \frac{\xi}{r}\cos\theta)\cos\psi, \quad I_s' = \int \frac{v d\tau}{R^3}(1 - \frac{\xi}{r}\cos\theta)\sin\psi.$$

Usually, this approximation is satisfied with a great accuracy. For example, for the observation sphere radius $r = 1m$ and the wavelength $\lambda = 4 \cdot 10^{-5} cm$, $kr$ is about $10^7$.

2. When the observation sphere radius $r$ is much larger than the motion interval, one can disregard the ratio $\xi/r$ everywhere except for the $\psi$ function. Then,

$$I_c = I_c' = \int v d\tau \cos\psi, \quad I_s = I_s' = \int v d\tau \sin\psi \quad \text{and}$$

$$\sigma(\theta,\omega) = \frac{d^2\mathcal{E}}{d\omega\Omega} = \frac{e^2\mu n k^2 \sin^2\theta}{4\pi^2 c}[(I_c)^2 + (I_s)^2]. \tag{2.2}$$

Usually, this condition is fulfilled in a majority of experiments.

3. The most serious approximation is $kL^2/r << \pi$ ($L$ is the motion interval). It arises from the fact that the development of the $k_n r(R-1)$ term occurring in $\psi$ has the form

$$k_n r(R-1) = -k_n \xi \cos\theta + \frac{k_n \xi^2 \sin^2\theta}{2r}.$$

The Tamm approximation is obtained when the last term in this expansion is neglected. This is possible, if it is much smaller than $\pi$ (since $\psi$ enters into sines and cosines). Then, $\psi$ takes the form

$$\psi = \omega\tau - kn\xi(\tau)\cos\theta. \tag{2.3}$$

In realistic conditions, this approximation is not satisfied. For example, for $\lambda = 4 \cdot 10^{-5} cm$, $L = 1cm$ and $r = 1m$, the discussed condition reduces to $400 << 1$, that is, it is greatly violated. The complications arising from the radiation intensity measurements at finite distances and the analytic formulae removing the above drawbacks were discussed in [11,12]. When the conditions 1-3 are fulfilled, the charge uniformly moving on the interval $(-z_0, z_0)$ radiates with the intensity given by the famous Tamm formula

$$\sigma_T(\theta,\omega) = \frac{e^2 \sin^2\theta}{\pi^2 nc}[\frac{\sin k_n z_0(\cos\theta - 1/\beta_n)}{\cos\theta - 1/\beta_n}]^2. \tag{2.4}$$

As an example, in Fig. 2 we present the Tamm radiation intensity (2.4) and the one taking account of a finite observation distance.

The aim of this consideration is to investigate the deviation from the Tamm formula (corresponding to infinite acceleration and deceleration at the beginning and end of motion) associated with smooth acceleration and deceleration of a charged particle. Although the evaluation according to (2.1) takes into account finite distances effects, but it obscures smooth acceleration effects, which we intend to study here. For this reason, we shall deliberately use (2.2) with $\psi$ given by (2.3).

# 3 Motion laws

We discuss the following two motion laws. The first of them is

$$v(t) = \frac{v_0}{ch^2(t/t_0)}. \tag{3.1}$$

Obviosly, $v(t) = v_0$ at $t = t_0$ and $v(t) \to 0$ for $t \to \pm\infty$. The charge position on the $z$ axis at the time $t$ is given by

$$\xi(t) = \int_0^t v(t)dt = v_0 t_0 \tanh\frac{t}{t_0}.$$

It is seen that $\xi = 0$ at $t = 0$ and $\xi(t) \to \pm v_0 t_0$ for $t \to \pm\infty$. Thus, $2v_0t_0 = L$, where $L$ is the motion interval. The dependences $v(t)$ and $v(\xi)$ are shown in Fig. 1 (b). The second motion law is

$$v(t) = v_0 \frac{1 + \cosh(t_1/t_0)}{\cosh(t_1/t_0) + \cosh(t/t_0)}. \tag{3.2}$$

Again, $v(t) = v_0$ at $t = t_0$ and $v(t) \to 0$ for $t \to \pm\infty$. The charge position on the $z$ axis at the time $t$ is given by

$$\xi(t) = \int_0^t v(t)dt = v_0 t_0 \coth(t_1/2t_0) \ln \frac{\cosh(t + t_1)/2t_0}{\cosh(t - t_1)/2t_0}.$$

It is seen that $\xi = 0$ at $t = 0$ and $\xi(t) \to \pm v_0 t_1 \coth t_1/2t_0)$ for $t \to \pm\infty$. Therefore, $2v_0t_1 \coth t_1/2t_0) = L$ where $L$ is the motion interval. The dependences $v(t)$ and $v(\xi)$ are shown in Fig. 1(c). It is seen that the ratio $t_1/t_0$, for the fixed $L$, defines the interval where $v \approx v_0$. This motion law is much richer than (3.1). It is widely used in nuclear physics to parametrize the nuclear densities [13,14].

# 4 Numerical results

Radiation intensities $\sigma$ corresponding to the motion law (3.1) for a number of $\beta_0 = v_0/c$ are shown in Fig. 3 side by side with the Tamm intensities $\sigma_T$ corresponding to the same $L, \beta_0$ and $\lambda$. It is seen that the positions of main maxima of $\sigma$ and $\sigma_T$ coincide for $\beta_0 > c_n$ and are at the Cherenkov angle defined by $\cos\theta_c = 1/\beta_0 n$. For $\beta_0 < c_n$, $\sigma$ is much smaller than $\sigma_T$. For $\theta > \theta_c$, $\sigma$ falls very rapidly and $\sigma_T$ dominates in this angular region. For $\theta < \theta_c$, $\sigma$ is much larger than $\sigma_T$.

To see how the measurements at finite distances affect the radiation intensities, we present, in Fig. 4, the radiation intensities corresponding to the motion law (3.1) and evaluated at finite distances. The general formula (2.1) valid at arbitrary distances was used for their evaluation. Side by side with them, shown are radiation intensities corresponding to the the uniform motion on the same interval and described by the Tamm formula (2.4). Comparing this figure with Fig. 2, we see that the modification of radiation intensities due to the finite distances is minimal for the motion law (3.1) and is essential for the Tamm problem (the origin of this discrepancy is not clear to us).

Radiation intensities $\sigma$ corresponding to the motion law (3.2) for fixed $v_0 = 1$, $L = 0.1cm$, $\lambda = 4 \cdot 10^{-5} cm$ and a number of diffuseness parameters $t_1/t_0$ are shown in Fig. 5 together with the Tamm intensities $\sigma_T$. The positions of main maxima are at the Cherenkov angle $\theta_c$. For small $t_1/t_0$, the main maximum of $\sigma$ is much higher than that of $\sigma_T$. They are approximately of the same height for $t_1/t_0 \geq 1$. Again, we observe that $\sigma$ falls almost instantly for $\theta > \theta_c$. On the other hand, $\sigma$ and $\sigma_T$ approach each other with rising $t_1/t_0$.

To see the influence of the value of the velocity $v_0$ at the origin, we evaluated radiation intensities for $t_1/t_0 = 10^{-3}$ fixed and various $v_0$. In this case, $v(t)$ is almost everywhere zero except for the neighbourhood of $t = 0$. We see (Fig. 6) that radiation intensities corresponding to (3.2) are much larger than the Tamm ones.

It is instructive to compare intensities corresponding to Fig. 1(a) with the Tamm intensities evaluated for the same $\beta_0$, $L$ and $\lambda$ (Fig. 7). The parameter $x_a$ is the ratio of the path on which a charge moves non-uniformly to the total path. For example, $x_a = 0.01$ means that a charge moves non-uniformly on the $1/100$ part of the total path. It is seen that for rather moderate acceleration paths ($x_a = 0.1$ and $x_a = .01$), the radiation intensities $\sigma$ fall rapidly for $\theta > \theta_c$. For smaller $x_a$, $\sigma$ and $\sigma_T$ approach each other (Fig. 7, c, d).

An important case is the motion with a final zero velocity. Experimentally, it is realized in heavy water reactors where electrons arising in $\beta$ decay are decelerated up to their complete stopping, in the original Cherenkov experiments (see below), etc. When the charge velocity is a linear function of time, the analytic solution in terms of Fresnel integrals was found in [10]. Radiation intensities for different initial velocities are shown in Fig. 8. It is easy to check that their maxima are always at the Cherenkov angle $\theta_1$ defined by $\cos\theta_1 = 1/\beta_1 n$ and corresponding to the initial velocity $v_1$. We conclude: the maximum of the radiation intensity at the Cherenkov angle does not necessarily testify to the charge uniform motion with $v > c_n$.
Despite the highly non-uniform character of this motiom, the main maximum of the radiation is at the Cherenkov angle $\theta_1$. Analytically, this will be proved in the next section. This means that under certain circumstances the bremsstrahlung can imitate the Cherenkov radiation.

An important characteristics is the total energy radiated per unit frequency. It is obtained by integration of the angular-frequency distribution over the solid angle:

$$\sigma_r(\omega) = \int \sigma_r(\omega, \theta) d\Omega. \tag{4.1}$$

The integration of the Tamm intensity (2.4) over the solid angle gives the frequency distribution of the radiated energy (see, e.g., [12])

$$\sigma_T(\omega) = \frac{d\mathcal{E}}{d\omega} = \int \sigma_T(\omega, \theta) d\Omega =$$

$$= \frac{2e^2\beta}{\pi c}(1 - \frac{1}{\beta_n^2})\{\frac{\sin^2\omega t_0(1-\beta_n)}{1-\beta_n} - \frac{\sin^2\omega t_0(1+\beta_n)}{1+\beta_n}$$
$$-\omega t_0[si(2\omega t_0(1-\beta_n)) - si(2\omega t_0(1+\beta_n))]\}-$$
$$-\frac{2e^2}{\pi c n\beta_n}[\ln\frac{|1-\beta_n|}{1+\beta_n} - ci(2\omega t_0|1-\beta_n|) + ci(2\omega t_0(1+\beta_n))]-$$
$$-\frac{e^2}{\pi c n\beta_n}\{2\beta_n + \frac{1}{2\omega t_0}[\sin 2\omega t_0(1-\beta_n)) - \sin 2\omega t_0(1+\beta_n))]\}. \tag{4.2}$$

Here $t_0 = z_0/v$, and $si(x)$ and $ci(x)$ are the integral sine and cosine. They are defined by the equations

$$si(x) = -\int_x^\infty \frac{\sin t}{t} dt, \quad ci(x) = -\int_x^\infty \frac{\cos t}{t} dt.$$

In the limit $\omega t_0 \to \infty$, (4.2) is transformed into the following expressions given by Tamm:

$$S_T(\omega) = \frac{2e^2 k z_0}{c}(1 - \frac{1}{\beta_n^2}) + \frac{4e^2}{\pi c n}(\frac{1}{2\beta_n} \ln \frac{1+\beta_n}{\beta_n - 1} - 1)$$

for $\beta_n > 1$ and

$$S_T(\omega) = \frac{4e^2}{\pi c n}(\frac{1}{2\beta_n} \ln \frac{1+\beta_n}{1-\beta_n} - 1) \tag{4.3}$$

for $\beta_n < 1$. Here $k = \omega/c$, $\beta_n = \beta n$, and $2z_0$ is the motion interval. Equation (4.3) has a singularity at $\beta = 1/n$, while (4.2) is not singular. To see how (4.2) and (4.3) agree with each other, we present them and their difference (Fig. 9 ) as a function of the velocity $\beta$ for typical parameters $L = 2z_0 = 0.1cm$ and $\lambda = 4 \cdot 10^{-5} cm$. We see that (4.2) and (4.3) coincide with each other everywhere except for the closest vicinity of $\beta = 1/n$.

We integrate now angular distributions shown in Fig. 8 and relate them to the Tamm integral intensitiy. Surprisingly, despite their quite different angular distributions, the ratio of integral intensities does not depend on the frequency (Fig. 10) except for the neighbourhood of $\beta = 1/n$ where (4.3) is not valid. For the charge velocity $v$ above the light velocity in medium $c_n$, this ratio decreases as $v$ approaches $c_n$. For $v < c_n$, this ratio begins to rise. Since decelerated integral intensities up to a factor independent of $\omega$ coincide with the Tamm one, the total energy for the decelerated motion

$$\mathcal{E} = \int_{\omega_1}^{\omega_2} d\omega \frac{d\mathcal{E}}{d\omega}$$

radiated in the frequency interval $(\omega_1, \omega_2)$ up to the same factor coincides with the Tamm integral intensity.

Numerical calculations of this section show that: 1) radiation intensities corresponding to Figs. 1(b) and (c) fall almost instantly for $\theta > \theta_c$. 2) For highly non-uniform motion with a zero final velocity, radiation intensity does not oscillates. Its maximum is at the Cherenkov angle corresponding to the initial charge velocity. This maximum shifts to larger angles with increasing initial velocity. 3) The integral intensity obtained by integration of the angular intensity is a linear function of the frequency (despite the highly non-uniform character of motion).

# 5 Analytic estimates

Let a charge move in the interval $(z_1, z_2)$ according to the motion law:

$$z = z_1 + v_1(t - t_1) + \frac{1}{2}a(t - t_1)^2. \tag{5.1}$$

The motion begins at the moment $t_1$ at the space point $z_1$ and terminates at the moment $t_2$ at the space point $z_2$. The charge velocity varies linearly with time from the value $v = v_1$ at $t = t_1$ up (or down) to value $v = v_2$ at $t = t_2$: $v = v_1 + a(t - t_1)$. It is convenient to express the acceleration $a$ and the motion interval through $z_1, z_2, v_1, v_2$:

$$a = \frac{v_1^2 - v_2^2}{2(z_1 - z_2)}, \quad t_2 - t_1 = \frac{2(z_2 - z_1)}{v_2 + v_1}.$$

When approximations (1-3) of section 3 are fulfilled (i.e., $\psi$ is of the form (2.3)), the integrals entering into (2.2) can be taken in a closed form [10]. Using them, we evaluate the intensity of radiation:

$$\sigma_r(\theta) = \frac{e^2k^2n\sin^2\theta}{4\pi^2c}[(\int_{z_1}^{z_2} dz' \cos\psi_1)^2 + (\int_{z_1}^{z_2} dz' \sin\psi_1)^2] =$$

$$= \frac{e^2\sin^2\theta}{2\pi^2cn\cos^2\theta}\{1 - \cos(u_2^2 - u_1^2) + \pi\alpha^2[(C_2 - C_1)^2 + (S_2 - S_1)^2] \pm$$

$$\pm\sqrt{2\pi}\alpha[(C_2 - C_1)(\sin u_2^2 - \sin u_1^2) - (S_2 - S_1)(\cos u_2^2 - \cos u_1^2)]\}, \tag{5.2}$$

where we put $C_1 = C(u_1)$, $C_2 = C(u_2)$, $S_1 = S(u_1)$, $S_2 = S(u_2)$,

$$\alpha = \sqrt{\frac{k(z_2 - z_1)}{n|\cos\theta(\beta_2^2 - \beta_1^2)|}}, \quad u_1 = \sqrt{\frac{k(z_2 - z_1)n|\cos\theta|}{|\beta_2^2 - \beta_1^2|}}(\beta_1 - \frac{1}{n\cos\theta}),$$

$$u_2 = \sqrt{\frac{k(z_2 - z_1)n|\cos\theta|}{|\beta_2^2 - \beta_1^2|}}(\beta_2 - \frac{1}{n\cos\theta});$$

$C$ and $S$ are the Fresnel integrals defined as

$$S(x) = \sqrt{\frac{2}{\pi}}\int_0^x dt \sin t^2 \quad \text{and} \quad C(x) = \sqrt{\frac{2}{\pi}}\int_0^x dt \cos t^2.$$

Plus and minus signs in (5.2) refer to $\cos\theta > 0$ and $\cos\theta < 0$, respectively. Further, $\beta_1 = v_1/c$ and $\beta_2 = v_2/c$. When $v_1 \to v_2 = v$, the radiation intensity (5.2) goes into the Tamm formula (2.4) in which one should put $z_0 = (z_2 - z_1)/2$.
Usually, the ratio of the motion interval to the observed wavelength is very large. In this case, one can change the Fresnel integrals by their asymptotic values:

$$C(x) \to \frac{1}{2} + \frac{\sin x^2}{\sqrt{2\pi}x}, \quad S(x) \to \frac{1}{2} - \frac{\cos x^2}{\sqrt{2\pi}x} \quad \text{for} \quad x \to +\infty \quad \text{and}$$

$$C(x) \to -\frac{1}{2} + \frac{\sin x^2}{\sqrt{2\pi}x}, \quad S(x) \to -\frac{1}{2} - \frac{\cos x^2}{\sqrt{2\pi}x} \quad \text{for} \quad x \to -\infty$$

(the fact that $C(-x) = -C(x)$ and $S(-x) = -S(x)$ was used).
For the motion corresponding to $\beta_1 n > 1$ and $\beta_2 n > 1$, one finds that for $k(z_2 - z_1) >> 1$, the radiation intensity is given by:

$$\sigma_r = \frac{e^2 n \sin^2\theta}{\pi^2 c}\{\frac{1}{4}[\frac{\beta_2 - \beta_1}{(1-\beta_1 n\cos\theta)(1-\beta_2 n\cos\theta)}]^2 + \\ + \frac{\beta_1\beta_2}{(1-\beta_1 n\cos\theta)(1-\beta_2 n\cos\theta)}\sin^2\frac{\psi}{2}\} \tag{5.3}$$

for $0 < \theta < \theta_2$ and $\theta > \theta_1$. Here we put

$$\cos\theta_1 = 1/\beta_1 n, \quad \cos\theta_2 = 1/\beta_2 n, \quad \psi = 2\frac{k(z_2 - z_1)}{\beta_1 + \beta_2}(\frac{\beta_1 + \beta_2}{2} n\cos\theta - 1).$$

On the other hand, for $\theta_2 < \theta < \theta_1$ one has

$$\sigma_r = \sigma_r(5.3) + \frac{e^2\sin^2\theta}{\pi c n\cos^2\theta}\{\alpha^2 + \frac{\alpha n\cos\theta}{\sqrt{2\pi}}[\beta_2\frac{\cos 2u_2}{\beta_2 n\cos\theta - 1} - \beta_1\frac{\cos 2u_1}{\beta_1 n\cos\theta - 1}]\}. \tag{5.4}$$

The term proportional to $\alpha^2$ is much larger than the first and last ones everywhere except for the angles close to $\theta_1$ and $\theta_2$. For these angles, the above expansion of Fresnel integrals fails (since $u_1$ and $u_2$ vanish at these angles). These formulae mean that the radiation intensity oscillates with decreasing amplitude for $0 < \theta < \theta_2$ and $\theta > \theta_1$ and decreases rather slowly like

$$\frac{e^2\alpha^2\sin^2\theta}{\pi c n\cos^2\theta} \tag{5.5}$$

for $\theta_2 < \theta < \theta_1$. The oscillating terms (first term in (5.4) and the term proportional to $\alpha$) are much smaller than (5.5). Exactly this behaviour of $\sigma_r$ with maxima at $\theta_1$ and $\theta_2$ and a rather flat region between them was stated in [10] where $\sigma_r$ was taken in the form (5.2). For $\beta_2 = 1/n$, the above formulae predict intensity oscillations for $\theta > \theta_1$ and their absence for $\theta < \theta_1$. Experimentally, the charge motion with deceleration is realized in Cherenkov experiments with heavy ions [15] where energy losses are essential due to their large atomic numbers. Formerly, analytic radiation intensities for the decelerated motion with the velocity change small as compared with the velocity itself were obtained in [11,16]. Numerically, decelerated motion with a large velocity change was studied in [6,17]. However, our experience tells us that pure numerical treatment of the problem without preliminary qualitative analysis is not very productive. It seems that this section fills this gap.

A particular interesting case having numerous practical applications corresponds to the complete termination of motion ($\beta_2 = 0$) . In this case,

$$\sigma_r = \frac{e^2 n\beta_1^2}{4\pi^2 c}\frac{\sin^2\theta}{(1-\beta_1 n\cos\theta)^2} \tag{5.6}$$

for $\theta > \theta_1$ and

$$\sigma_r = \sigma_r(5.6) + \frac{e^2 \sin^2\theta}{\pi c n \cos^2\theta}[\alpha^2 - \frac{\beta_1 \alpha n \cos\theta}{\sqrt{2\pi}} \frac{\cos 2u_1}{\beta_1 n \cos\theta - 1}] \tag{5.7}$$

for $\theta < \theta_1$. Here

$$\alpha = \frac{1}{\beta_1}\sqrt{\frac{k(z_2 - z_1)}{n\cos\theta}}, \quad u_1 = \sqrt{k(z_2 - z_1)n\cos\theta}(1 - \frac{1}{\beta_1 n \cos\theta}).$$

There are no intensity oscillations (since $\alpha >> 1$ and, therefore, $\alpha^2 >> \alpha$) for $\theta > \theta_1$ and they are very small oscillations for $\theta < \theta_1$ (they are due to the last term in (5.7)). Figure 8 agrees with this prediction.

We clarify now why the radiation intensities disappear for $\theta > \theta_c$ for the motion shown in Fig. 1 (a). For this aim, we should evaluate the integrals $I_c = \int v d\tau \cos\psi$ and $I_s = \int v d\tau \sin\psi$ entering into (2.2). For $\psi$ in the form (2.3), $I_s$=0 due to the symmetry of the treated problem. Then, $I_c$ is reduced to

$$I_c = I_c^a + I_c^d + I_c^u = 2I_c^a + I_c^u. \tag{5.8}$$

Here $I_c^a$, $I_c^d$, and $I_c^u$ are integrals over the accelerated ($-z_0 < z < -z_1$), decelerated ($z_1 < z < z_0$) and uniform ($-z_1 < z < z_1$) parts of a charge trajectory, respectively. Again, it was taken into account that $I_c^a = I_c^d$ due to the symmetry of the problem. The integral $I_c^u$ corresponding to the uniform motion on the interval ($-z_1 < z < z_1$) is

$$I_c^u = \frac{2\beta}{k(1 - \beta n \cos\theta)} \sin[\frac{kz_1}{\beta}(1 - \beta n \cos\theta)] \ . \tag{5.9}$$

Then, for $\theta < \pi/2$, one gets

$$I_c^a = \int_{-z_0}^{-z_1} dz \cos\psi = \frac{1}{kn\cos\theta}\{\sin(u_2^2 - \gamma) - \sin(u_1^2 - \gamma) +$$

$$\alpha\sqrt{2\pi}[\cos\gamma(C_2 - C_1) + \sin\gamma(S_2 - S_1)]\}. \tag{5.10}$$

For the motion shown in Fig.1 (a), $u_1$, $u_2$, $\alpha$, and $\gamma$ are given by

$$u_1 = -\sqrt{k(z_0 - z_1)n\cos\theta}\frac{1}{\beta n\cos\theta}, \quad u_2 = \sqrt{k(z_0 - z_1)n\cos\theta}(1 - \frac{1}{\beta n\cos\theta}),$$

$$\alpha = \frac{1}{\beta}[\frac{k(z_0 - z_1)}{n\cos\theta}]^{1/2}, \quad \gamma = kz_0 n\cos\theta + \frac{k(z_0 - z_1)}{\beta^2 n\cos\theta} - \frac{k(2z_0 - z_1)}{\beta}.$$

Changing Fresnel integrals by their asymptotic values, we get for $k(z_0 - z_1) >> 1$ and $\theta < \theta_c$ ($\cos\theta_c = 1/\beta n$):

$$C_2 - C_1 = -1 + \frac{1}{\sqrt{2\pi}}(\frac{\sin u_2^2}{u_2} - \frac{\sin u_1^2}{u_1}), \quad S_2 - S_1 = -1 - \frac{1}{\sqrt{2\pi}}(\frac{\cos u_2^2}{u_2} - \frac{\cos u_1^2}{u_1}).$$

Substituting this into (5.10), we get

$$I_c^a = -\alpha\sqrt{2\pi}\frac{\cos\gamma + \sin\gamma}{kn\cos\theta} + \frac{\beta n}{k(\beta n\cos\theta - 1)}\sin[kz_1(1-\beta n\cos\theta)]. \qquad (5.11)$$

To obtain $I_c$, one should double $I_c^a$ (since $I_c^a = I_c^d$) and add $I_c^u$ given by (5.9). This gives

$$I_c = 2I_c^a + I_c^u = -\alpha\sqrt{2\pi}\frac{\cos\gamma + \sin\gamma}{kn\cos\theta} \quad \text{and}$$

$$\sigma_r = \frac{e^2}{2\pi cn^2\beta^2}k(z_0 - z_1)\frac{\sin^2\theta}{\cos^3\theta}(1 + \sin 2\gamma). \qquad (5.12)$$

We see that for $\theta < \theta_c$ the part of $I_c^a$ is compensated by the Tamm amplitude $I_c^u$. In this angular region the oscillations are due to the $(1 + \sin 2\gamma)$ factor.

For $\theta > \theta_c$, one obtains

$$C_2 - C_1 = \frac{1}{\sqrt{2\pi}}(\frac{\sin u_2^2}{u_2} - \frac{\sin u_1^2}{u_1}), \quad S_2 - S_1 = -\frac{1}{\sqrt{2\pi}}(\frac{\cos u_2^2}{u_2} - \frac{\cos u_1^2}{u_1}).$$

Substituting this into (5.10), we get

$$I_c^a = \frac{\beta n}{k(\beta n\cos\theta - 1)}\sin[kz_1(1-\beta n\cos\theta)]. \qquad (5.13)$$

Inserting (5.9) and (5.13) into (5.8), one finds

$$I_c = 2I_c^a + I_c^u = 0.$$

We see that for $\theta > \theta_c$ the summary contribution of the accelerated and decelerated parts of the charge trajectory is compensated by the contribution of its uniform part. The next terms arising from the expansion of the Fresnel integrals are of the order $1/k(z_0 - z_1)$ and, therefore, are negligible for $k(z_0 - z_1) >> 1$. This behaviour of radiation intensities is confirmed by Figs. 5 - 7.

The radiation intensity for $\theta > \theta_c$ disappears for arbitrary $z_1$ satisfying the conditon $z_0 - z_1 >> 1$ and, in particular, for $z_1 = 0$. In this case, there is no uniform motion, and accelerated motion on the interval $-z_0 < z < 0$ is followed by the decelerated motion on the interval $0 < z < z_0$. Equations (5.12) and (5.13) with $z_1 = 0$ in them qualitatively describe Figs. 3 and 6 corresponding to a small length of uniform motion.

It should be stressed again that these estimates are not valid near the angles $\theta_1$ and $\theta_2$ where the arguments of the Fresnel integrals vanish.

# 6 Discussion

As we have mentioned in the Introduction, P.A. Cherenkov being at first the follower of Vavilov's explanation of the nature of radiation observed in his experiments later

changed his opinion in favour of the Tamm-Frank theory. What are the reasons for this?

At first we clarify conditions under which the Cherenkov experiments were performed. According to him, "... the absorption of electrons in fluids was complete." ([7], p.24). This means that we should apply numerical and analytic results of sections 4 and 5 corresponding to the charge motion with a zero final velocity.

There are three main reasons why Cherenkov abandoned the original viewpoint. We concern them step by step.

1. "For the radiation produced by electrons in fluids, the angle $\theta$ (counted from the direction of the electron motion) for which the maximum of radiation is observed increases with increasing electron velocity. This dependence of $\theta$ is just opposite to that expected if one suggests that radiation of fluids is due to deceleration. For the bremsstrahlung it is characteristic that the position of the intensity maximum shifts towards the initial beam with rising electron energy" ([7], p.33).
However, numerical and analytic results of sections 4 and 5 and Fig. 8 demonstrate that the maximum of the intensity behaves for the decelerated motion exactly in the same way as in the Tamm-Frank theory.

2. On the fall of the radiation intensity at large angles. Again, we quote P.A. Cherenkov: " To the aforesaid about the azimuthal distribution of the intensity should be added that the asymmetry of radiation relative to the plane perpendicular to the electron beam is more pronounced for the observed radiation of fluids than for the bremsstrahlung" ([7], p.34).
Turning to the motion laws presented in Fig.1, it was shown numerically and analytically in sections 4 and 5 that the radiation intensity falls more rapidly than that described by the Tamm formula. For the decelerated motion with a zero final velocity, the falling of radiation is determined either by exact equation (5.2) (where one should put $\beta_2 = 0$) or by analytic Eq. (5.7). The latter is infinite at $\cos\theta = 1/\beta n$, while (5.2) gives $\sigma_r(\cos\theta = 1/\beta n) = e^2 Ln(1 - 1/\beta_n^2)/2c\lambda$ ($L$ and $\lambda$ are the motion interval and wavelength). The Tamm intensity at the same angle is much larger for $L/\lambda >> 1$: $\sigma_T(\cos\theta = 1/\beta n) = e^2 L^2 n(1 - 1/\beta_n^2)/c\lambda^2$ Comparing (2.4) and (5.7) we see that for $\theta > \theta_c$, $\sigma_r$ and $\sigma_T$ decrease in the same way with the exception that $\sigma_T$ oscillates, while $\sigma_r$ does not (Fig. 8). It should be mentioned that there were no angular intensity oscillations in original Cherenkov experiments.

3. The last Cherenkov objection concerns the frequency dependence of the integral intensity. Accordimg to him "In both the cases, the same qualitative result is obtained: the energy of the bremsstrahlung spectrum decreases at large frequencies. For our purposes, it is enough to say that it does not rise with energy. On the other hand, the experiment shows that, for the radiation induced by fast electrons, the energy rises in proportion to the frequency, which, obviously, disagrees with results following from the bremsstrahlung theory" ([7], p.33).
Turning to Fig. 10, we observe that the ratio of the bremsstrahlung integral intensity to that of Tamm does not depend on the frequency. Since the Tamm integral intensity rises in proportion to the frequency, the same is valid for the bremsstrahlung integral intensity.

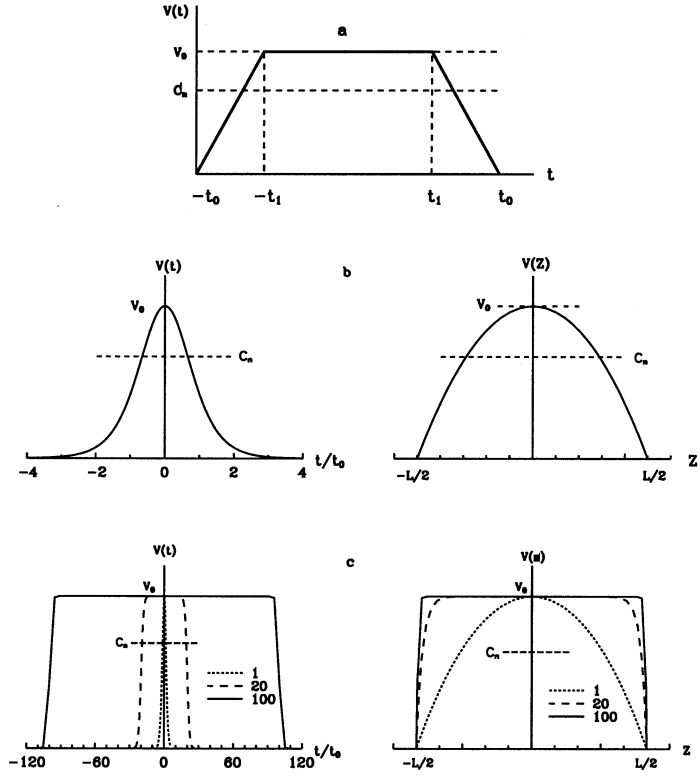


Fig. 1: Three types of motion considered in the text.
(a) Superposition of accelerated ($-t_0 < t < -t_1$), uniform ($-t_1 < t < t_1$), and decelerated ($t_1 < t < t_0$) motions. The drawback of this motion is due to the acceleration jumps at $t = \pm t_0$ and $t = \pm t_1$.
(b) The motion corresponding to $v(t) = v_0/ch^2(t/t_0)$. Left and right parts correspond to $v(t)$ and $v(\xi)$ where $\xi$ is the charge position ($\xi(t) = \int_0^t v(t)dt$) at the time $t$. It is seen that the charge position is confined to a finite space interval $(-L/2, L/2)$.
(c) The motion corresponding to $v(t) = v_0[1+\cosh(t_1/t_0)]/[\cosh(t/t_0)+\cosh(t_1/t_0)]$. For large $t_1/t_0$, the interval corresponding to the motion with a constant velocity increases. The charge position is confined to a finite space interval $(-L/2, L/2)$. This motion is much richer than (b).

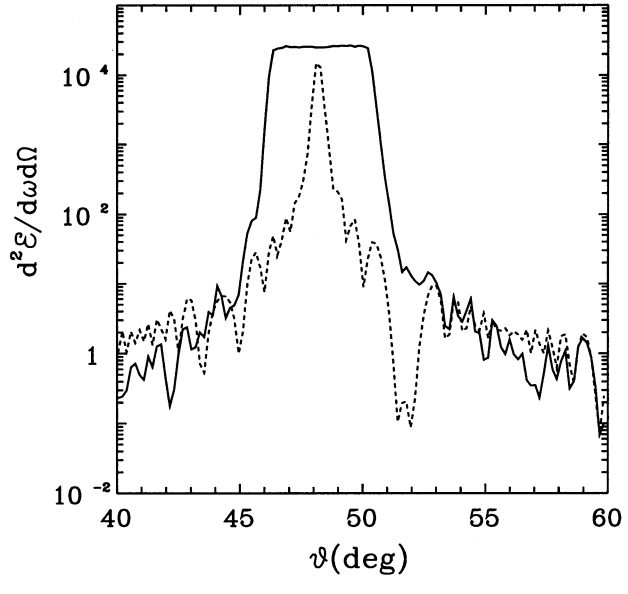


Fig. 2: Angular radiation intensities (in units $e^2/c$) corresponding to the charge motion on a finite interval (Tamm problem). The solid and dotted lines correspond to the radii of the observation sphere $r = 1cm$ and $r = \infty$. The latter intensity is decribed by the Tamm formula (2.4). The original angular intensities are highly oscillating functions. To make them more visible, we average them over three neighbouring points, thus, considerably smoothing the oscillations. This is valid for Figs. 2-7. The charge velocity is $\beta_0 = 1$, the motion interval $L = 0.1cm$, the wavelength $\lambda = 4 \cdot 10^{-5} cm$, the refractive index $n = 1.5$. The last three parameters are the same for all subsequent figures.

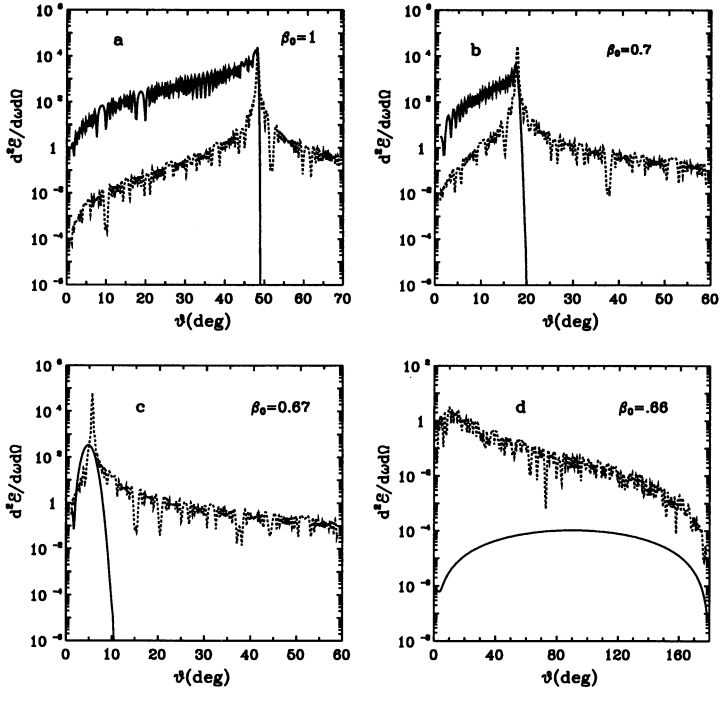


Fig. 3: Angular radiation intensities corresponding to the charge motion shown in Fig. 1 (b) (solid curves) and the Tamm intensities (dotted lines) for various values of $v_0$. For $v_0 > c_n$, the maximum of intensity is at the Cherenkov angle $\theta_c$ defined by $\cos\theta_c = 1/\beta_0 n$. The angle $\theta_c$ decreases with decreasing $v_0$. For $\theta > \theta_c$ and $\beta_0 > 1/n$, the radiation intensity falls almost instantly. This is explained analytically in section 5.

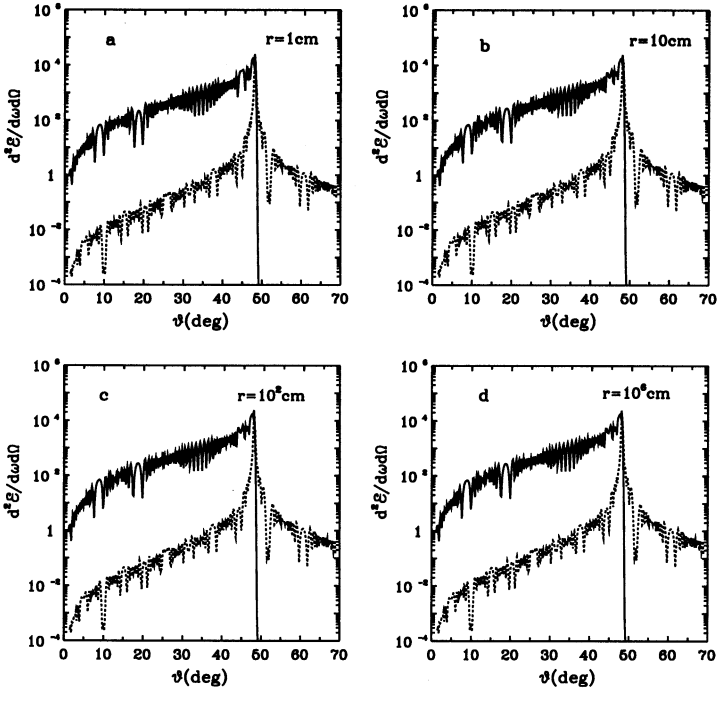


Fig. 4: Angular radiation intensities corresponding to the charge motion shown in Fig. 1 (b) for $\beta_0 = 1$ and various radii $r$ of the observation sphere (solid curves) and the Tamm intensities (dotted lines). It is seen that angular intensities are almost the same for any $r$. This is contrasted with the drastic $r$ dependence of angular intensities corresponding to the uniform motion (see Fig.2).

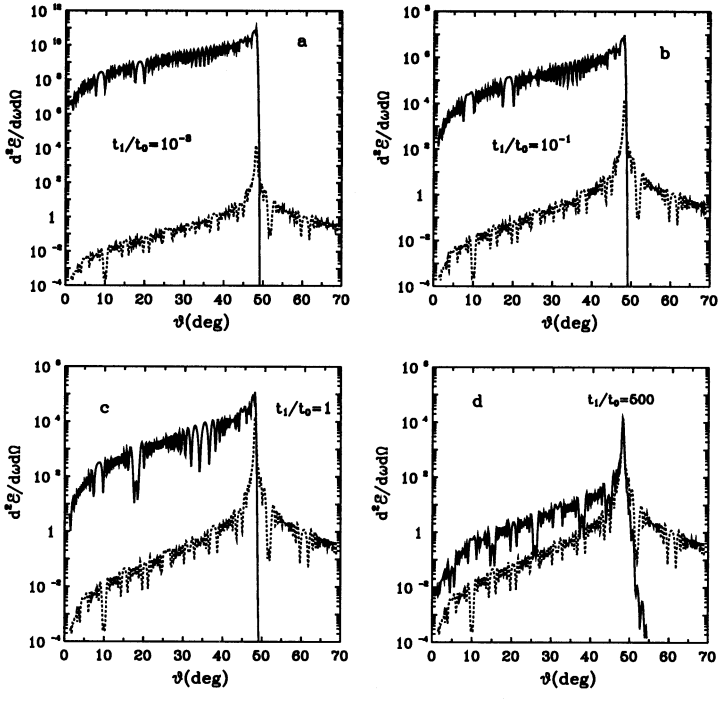


Fig. 5: Angular radiation intensities corresponding to the charge motion shown in Fig. 1 (c) (solid lines) for $\beta_0 = 1$ and a number of diffuseness parameters $t_1/t_0$. Angular intensities approach the Tamm one (dotted line) for large values of $t_1/t_0$.

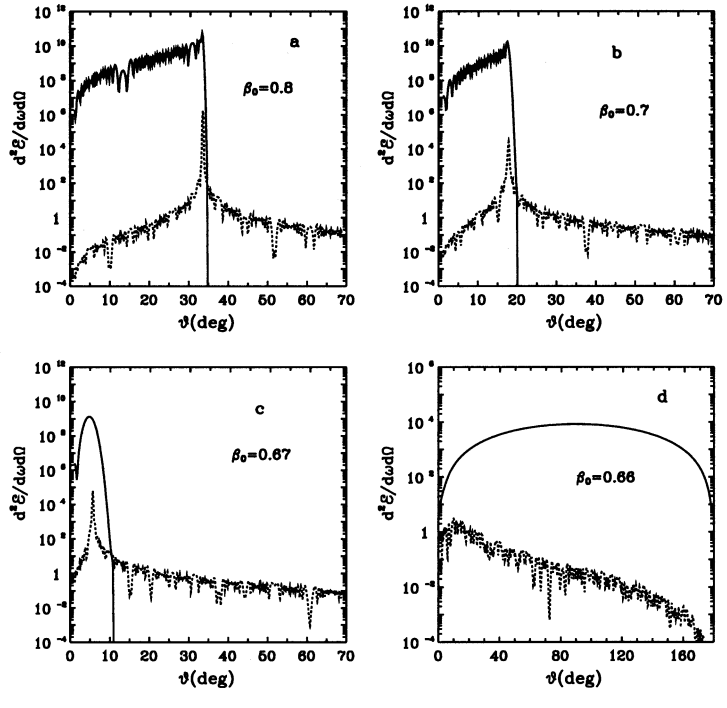


Fig. 6: Angular radiation intensities corresponding to the charge motion shown in Fig. 1 (c) (solid curves) for $t_1/t_0 = 10^{-3}$ and a number of velocities $v_0$. These intensities are much larger than the Tamm ones (dotted curves).

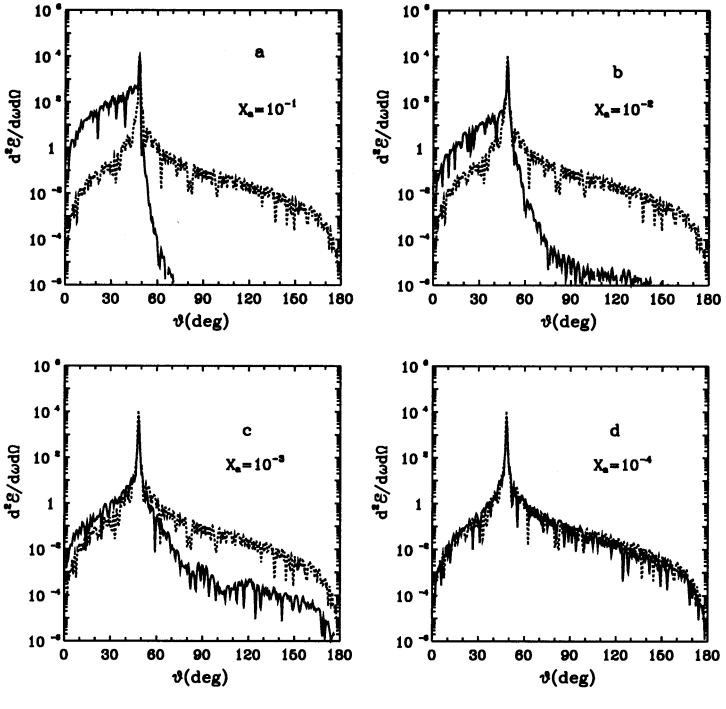


Fig. 7: Angular radiation intensities (solid curves) corresponding to the charge motion shown in Fig. 1 (a) for $\beta_0 = 1$ and a number of non-uniform motion lengths. Here $x_a$ is the ratio of the path where a charge moves non-uniformy to the total path. It is seen that angular radiation intensities approach the Tamm one (dotted curves) when $x_a \to 0$.

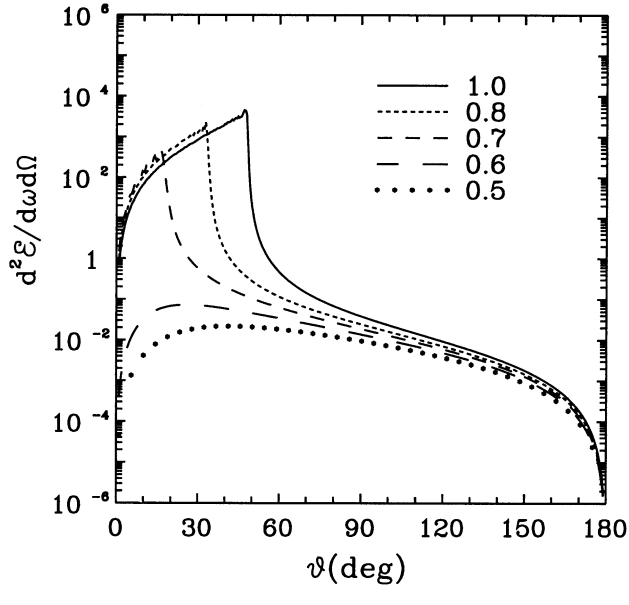


Fig. 8: Angular radiation intensities corresponding to the charge motion with its complete stopping for a number of initial velocities. It is seen that these intensities do not oscillate. The angle where they are maximal increases with increasing of the initial velocity $\beta_1$. Numbers at curves mean $\beta_1$.

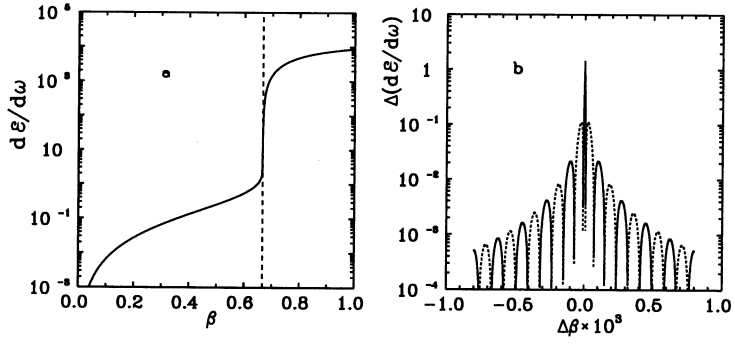


Fig. 9: (a) Frequency distributions of the radiated energy (in $e^2/c$ units) evaluated according to (4.2) and its simplified version (4.3) as functions of the charge velocity. They are indistinguishable on this scale; (b) the difference between (4.3) and (4.2). The regions where this difference is negative are shown by dotted lines; $\delta\beta$ means $\beta - 1/n$. .

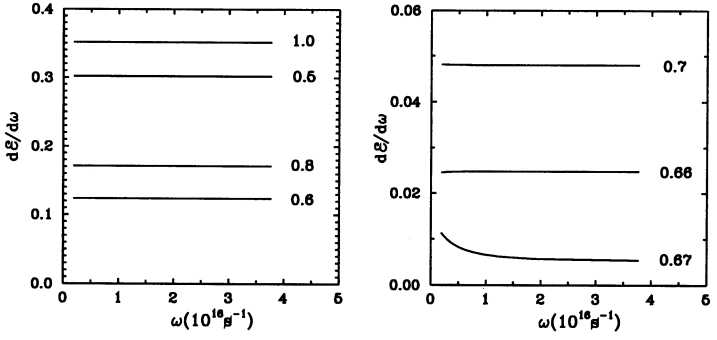


Fig. 10: The ratio of the integral intensity for the motion with a zero final velocity to the Tamm integral intensity (4.3) for a number of initial velocities $v_1$. Although this ratio does not depend on the frequency (except for the velocity $\beta_1 = 0.67$ close to the Cherenkov threshold $1/n$), it strongly depends on $\beta_1$ being minimal at the threshold. To this frequency interval there corresponds the wavelength interval $(5 \cdot 10^{-6} cm < \lambda < 10^{-4} cm)$ which encompasses the visible light interval $(4 \cdot 10^{-5} cm < \lambda < 8 \cdot 10^{-5} cm)$.

We summarize the discussion: it seems that the radiation observed in original Cherenkov experiments is due to the decelerated electrons. Vavilov's explanation of these experiments supported initially by Cherenkov was correct. Probably, the beauty of the Tamm-Frank theory concretely predicting the position of the radiation maximum, its dependence on the electron energy and the medium properties, frequency proportionality of the total radiated energy, the absence of concrete calculations on the radiation of decelerated electron in medium (Cherenkov used references treating bremsstrahlung in vacuum), and the similarity of the predictions of the Tamm-Frank theory and bremsstrahlung theory in medium, enabled him to change his opinion.

Aforesaid is related to the original Cherenkov experiments where the Compton electrons knocked out by photons are completely absorbed in medium. In modern experiments, high energy charged particles move through a medium almost without energy loss. In this case, one can use either the original Tamm formula (2.4) or its modification for finite observation distances [11].

# 7 Conclusion

1. We have evaluated radiation intensity for the Tamm problem with absolute continuous time dependence of a charge velocity. It is shown that the radiation intensity is described by the Tamm problem when the length of acceleration region tends to zero.
2. We have shown that the fact that the maximum of the radiation intensity lies at the Cherenkov angle does not necessarily indicate the charge uniform motion with a velocity greater than the large velocity in medium. In fact, we have shown numerically and analytically that the maximum of the radiation intensity lies at the Cherenkov angle even if the motion is highly non-uniform.
3. It is shown for the motion beginning with the velocity $v_1$ and terminating with the velocity $v_2$, that there are two Cherenkov maxima if both $\beta_1 n$ and $\beta_2 n$ are greater than 1. Only one Cherenkov maximum survives if one of these quantities is smaller than 1.
4. The radiation intensity for the charge completely stopping in a medium does oscillate. Its maximum is at the Cherenkov angle $\theta_c$ defined by $\cos\theta_c = 1/\beta n$ where $\beta$ is the initial velocity. The integral intensity is a linear function of frequency.

# References


[1] Vavilov S.I., 1934, Dokl. Akad, Nauk, 2, 8, 457.

[2] Cherenkov P.A., 1936, Dokl. Akad, Nauk, 3, 9, 413.

[3] Frank I.M., 1988, Vavilov-Cherenkov Radiation (Moscow, Nauka), In Russian.

[4] Tamm I.E., 1939, J.Phys. USSR, 1, 439.

[5] Afanasiev G.N., Eliseev S.M. and Stepanovsky Yu.P., 1998, Proc. Roy. Soc. Lond. A, 454, 1049; Afanasiev G.N. and Kartavenko V.G., 1999, Can. J. Phys., 77, 561.

[6] Afanasiev G.N. and Shilov V.M., 2000, Physica Scripta, 63, 326.

[7] Cherenkov P.A., 1944, Trudy FIAN, 2, No 4, 3.

[8] Zrelov V.P., Ruzicka J., 1989, Chech.J.Phys. B, 39, 368.

[9] Zrelov V.P., Ruzicka J., 1992, Chech.J.Phys., 42, 45.

[10] Afanasiev G.N. and Shilov V.M., 2001 (submitted to Journal of Physics D: Applied Physics); Preprint JINR, E2-2002-36, Dubna, 2002.

[11] Afanasiev G.N. and Shilov V.M., 2000, J. Phys.D, 33, 2931.

[12] Afanasiev G.N., Kartavenko V.G. and Ruzicka J., 2000, J. Phys. A, 33, 7585.

[13] Lukyanov V.K., Eldyshev Yu.N. and Pol' Yu.S., 1973, Sov. J. Nucl. Phys., 16, 282.

[14] Grypeos M.E., Koutroulos G., Lukyanov V.K. and Shebeko A.V., 2001, Particles and Nuclei, 32, 1494.

[15] Ruzicka J. et al., 2000, Nucl. Instr. Methods,A, 431, 148.

[16] Kuzmin E.S. and Tarasov A.V., 1993, JINR Rapid Communications, 4[61]-93, 64, Dubna, 1993.

[17] Krupa L., Ruzicka J. and Zrelov V.P., 1995, JINR Preprint P2-95-281, Dubna, 1995

Received on March 5, 2002.

Афанасьев Г. Н. и др. Е2-2002-37
Численное и аналитическое рассмотрение
сглаженной задачи Тамма

Рассматривается движение заряда в среде на конечном интервале. Движение описывается абсолютно непрерывными функциями времени (это означает, что непрерывны не только скорости, но и все их производные по времени). Для сглаженной задачи Тамма интенсивность излучения резко убывает при углах, превышающих черенковский. Аналитически показано, что это связано с взаимной компенсацией вкладов равномерного и ускоренного движений. В важном для применений случае, соответствующем нулевой конечной скорости, интенсивность излучения максимальна при черенковском угле, соответствующем начальной скорости. Интегральная интенсивность (полученная интегрированием углового распределения по телесному углу) является линейной функцией частоты. Эти результаты применяются к первоначальным экспериментам Черенкова с полным поглощением комптоновских электронов в воде.

Работа выполнена в Лаборатории теоретической физики им. Н. Н. Боголюбова ОИЯИ.

Препринт Объединенного института ядерных исследований. Дубна, 2002

Afanasiev G. N. et al. E2-2002-37
Numerical and Analytic Treatment of the Smoothed Tamm Problem

We consider the charge motion in medium in a finite space interval. This motion is described by absolutely continuous functions of time (this means that not only functions themselves but all their time derivatives are continuous as well). For the smoothed Tamm problem, the radiation intensity suddenly drops for the angles exceeding the Cherenkov angle. It is shown analytically that this is due to the fact that contributions of accelerated and uniform motions to the radiation intensity cancel each other. In a practically important case corresponding to the zero final charge velocity, the radiation intensity is maximal at the Cherenkov angle corresponding to the initial charge velocity. The integral intensity corresponding to this motion (obtained by integration of the angular radiation intensity over the solid angle) is a linear function of frequency. These results are applied to the original Cherenkov experiments corresponding to the complete absorption of Compton electrons in water.

The investigation has been performed at the Bogoliubov Laboratory of Theoretical Physics, JINR.

Preprint of the Joint Institute for Nuclear Research. Dubna, 2002

Макет *Т. Е. Попеко*

ЛР № 020579 от 23.06.97.
Подписано в печать 15.03.2002.
Формат 60 × 90/16. Бумага офсетная. Печать офсетная.
Усл. печ. л. 1,68. Уч.-изд. л. 2,63. Тираж 425 экз. Заказ № 53175.

Издательский отдел Объединенного института ядерных исследований
141980, г. Дубна, Московская обл., ул. Жолио-Кюри, 6.